

Generalized compound synchronization of chaos in different orders chaotic Josephson junctions

K. S. Ojo · A. N. Njah · O. I. Olusola

Received: 10 May 2014 / Accepted: 25 July 2014
© Springer-Verlag Berlin Heidelberg 2014

Abstract This paper investigates compound synchronization scheme between three drive Josephson junctions and one response Josephson junction of a different order via the active backstepping technique. Reduced-order projective compound synchronization and anti-synchronization as well as reduced order hybrid projective synchronization between three third order Josephson junctions and one second order Josephson junction are considered. In each case, sufficient conditions for global asymptotic stability for generalized compound synchronization of different Josephson junctions are achieved via the active backstepping technique. Numerical simulations are performed to validate the effectiveness of the proposed synchronization scheme. The result shows that this scheme could be used to vary the junction signal to any desired level and also give a better insight into synchronization in biological systems wherein different organs of different dynamical structures and orders are involved. The scheme could also provide high security in information transmission due to the complexity of its dynamical formulation.

Keywords Reduced-order compound synchronization · Josephson junction · Backstepping technique

1 Introduction

Josephson junction is a very important nonlinear system which has attracted great attention due to its advantage in

devices that require ultra low noise, low power consumption, and high working frequency [1]. Based on the rapid development of superconducting devices in the fabrication technology different models of Josephson junction have been reviewed in order to understand whether such superconducting junction can be used as transmitter and receiver in chaotic digital communication [2]. Among these models are the shunted linear resistive-capacitive junction RCSJ [3], the shunted nonlinear resistive-capacitive junction SNRCJ [4], the shunted nonlinear resistive-capacitive-inductance junction RCLSJ [5] and the periodically modulated Josephson junction PMJJ [6]. Chaos in superconducting Josephson junction has been studied extensively by many researchers [2, 7–10]. Interest in complex dynamics of Josephson junctions have been extended to large arrays of coupled Josephson junctions since such arrays of coupled Josephson junctions can generate large power output in the millimeter and sub-millimeter wave ranges [11]. Synchronization of the superconducting junction arrays is also important for the purpose of generating reasonably large output power [12].

Synchronization between coupled chaotic systems gives better insight for understanding the collective behaviour of nonlinear systems [13]. Synchronization and control of coupled chaotic systems have been widely investigated due to their potential applications in many fields such as neural networks, biological networks, secure communication etc. As a result of the diversity and complexity of dynamical behaviours of real complex systems, many kinds of synchronization types and schemes have been developed and investigated, such as complete synchronization [14], anti-synchronization [15], hybrid synchronization [16], projective synchronization [17], projective hybrid synchronization [18], reduced-order synchronization [19], increased order synchronization [20], function projective synchronization [21] combination synchronization [22, 23], combination-combination synchro-

K. S. Ojo (✉) · O. I. Olusola
Department of Physics, University of Agriculture, Abeokuta,
Nigeria
e-mail: kaystephe@yahoo.com; kaojo@unilag.edu.ng

K. S. Ojo · A. N. Njah
Department of Physics, University of Lagos, Lagos, Nigeria

nization [24,25], Compound synchronization [26] and so on. Meanwhile, many chaos control and synchronization methods have been proposed to design proper controllers, including feedback control method, adaptive control, active control, open-plus-closed-loop, backstepping, sliding mode control etc [27–32].

Projective synchronization is achieved when the responses of two or more systems synchronize up to a constant positive scaling factor $\alpha \in \mathbb{R}$ [33]. While, Projective anti-synchronization is achieved when the responses of two or more systems synchronize up to a constant negative scaling factor so complete synchronization and anti-synchronization can be regarded as the special cases of projective synchronization and projective anti-synchronization with $\alpha = 1$ and $\alpha = -1$ respectively. In general, Projective synchronization has been extensively studied because faster communication can be realized with its proportional feature [16]. Meanwhile, Hybrid synchronization scheme is a synchronization scheme wherein one part of the system is anti-synchronized and the other part completely synchronized such that complete synchronization and anti-synchronization co-exist in the system [16]. The co-existence of complete synchronization and anti-synchronization enhances security in communication and chaotic encryption schemes. Hybrid projective synchronization is a synchronization scheme wherein one part of the system synchronizes up to a constant positive scaling factor $\alpha \neq 1$ while, the other part of the system synchronizes up to a constant negative scaling factor $\alpha \neq -1$ so, projective hybrid synchronization is a combination of hybrid and projective synchronization. The realization of synchronization and anti-synchronization in a chaotic secure communication scheme could give additional security advantage to information transmission.

Most of the aforementioned works are based on the synchronization scheme which consists of only one drive system and one response system with, thus, limit the flexibility and applicability to real world systems such as in secure communication [25]. Recently, combination synchronization which involves two drive systems and one response system was investigated [22,23]. Also, combination-combination synchronization, where synchronization is achieved between two drive systems and two response systems was implemented, [24,25]. This recently developed synchronization scheme can improve the security of information transmission for example, information signal can be divided into several parts, then each part loaded in each of the different drive systems, and after transmission the original signals is retrieved by combining the received signals of different response systems correctly. Meanwhile, in 2013 a novel synchronization scheme called compound synchronization scheme which gives a better security in information transmission was proposed and implemented for four chaotic memristors with application to secure communication [26]. The novel com-

pound synchronization realized chaos synchronization by multiplication and addition of multiple chaotic systems while the combination or combination-combination synchronization scheme was realized by simple addition or subtraction of multiple chaotic systems. This novel compound synchronization scheme gives higher level of security to information transmission due to the complexity of the drive dynamical systems and the formation of the drive signal as well as the modulation technique used [26]. To the best of our knowledge, this important compound synchronization has not been investigated for chaotic systems of different orders. So, in this paper we report compound synchronization of chaotic systems of different orders for the first time.

On the other hand, synchronization between drive and response systems with different order which is ubiquitous in many physical and biological systems has not been adequately investigated [23,34,35]. Studies on the cardiorespiratory system has shown that such a synchronization phenomenon occurs between heart and lung [35]. That is to say, the circulatory and respiratory systems behave in a synchronous way, even though their models have different dynamical systems and orders. Furthermore, chaotic synchronization of chaotic systems with different orders have been applied in secure communication [36] Hence, compound synchronization of different order nonlinear chaotic systems deserved to be investigated in view of its practical applications in biological systems and secure communication.

The rest of this paper is organized as follows. Section 2 gives the system description. Sections 3 deals with reduced-order compound synchronization scheme. Section 4 examines generalized reduced-order compound synchronization of three third order and one second order chaotic Josephson junctions and Sect. 5 concludes the paper.

2 Description of Josephson junctions

2.1 Resistive-capacitive-inductive shunted Josephson junction (RCLSJJ)

The resistive-capacitive-inductive shunted Josephson junction in dimensionless form is described by the set of first order differential equations below

$$\begin{aligned}\dot{x} &= y \\ \dot{y} &= \frac{1}{\beta_C}(i - g(y)y - \sin x - z) \\ \dot{z} &= \frac{1}{\beta_L}(y - z)\end{aligned}\quad (1)$$

where $g(y)$ is the nonlinear damping function approximated by current-voltage relation between the junctions and is

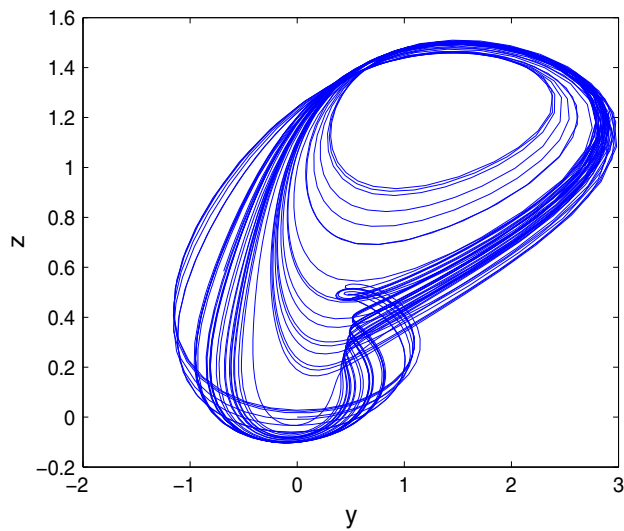


Fig. 1 Phase portrait of chaotic attractors of resistive-capacitive-inductive Josephson junction

defined by

$$g(y) = \begin{cases} 0.366 & \text{if } |y| > 2.9 \\ 0.061 & \text{if } |y| \leq 2.9 \end{cases}$$

x , y and z represent the phase difference, the voltage in the junction and the inductive current respectively. β_C and β_L are capacitive and inductive constant respectively. i is the external direct current. Figure 1 shows the chaotic attractor of the RCL shunted Josephson junction for the following set of parameters: $i = 1 < i < 1.3$, $\beta_C = 2.6$ and $\beta_L = 0.707$ with the initial conditions $(x, y, z) = (0, 0, 0)$. The RCL shunted Josephson has been found to be more appropriate in high frequency applications. In RCL Josephson junction chaotic oscillation has modulated in response to both the amplitude and frequency of an external sinusoidal signal.

2.2 Resistive-capacitive shunted Josephson junction (RCSJJ)

The resistive-capacitive Josephson junction under the external periodic force is given by the second order differential equation below

$$\ddot{\phi} = -\alpha\dot{\phi} - \sin \phi + a + b \sin \omega t \quad (2)$$

where ϕ is the phase difference between quantum mechanical wave function of two superconductors junction separated by some non-superconducting material or barrier. α and a are the dimensionless damping and applied current. $b \sin \omega t$ is the external periodic sinusoidal force. b and ω respectively are the amplitude and frequency of the external periodic sinusoidal force. The second order differential equation in (2) can be transformed into a set of first order differential equation

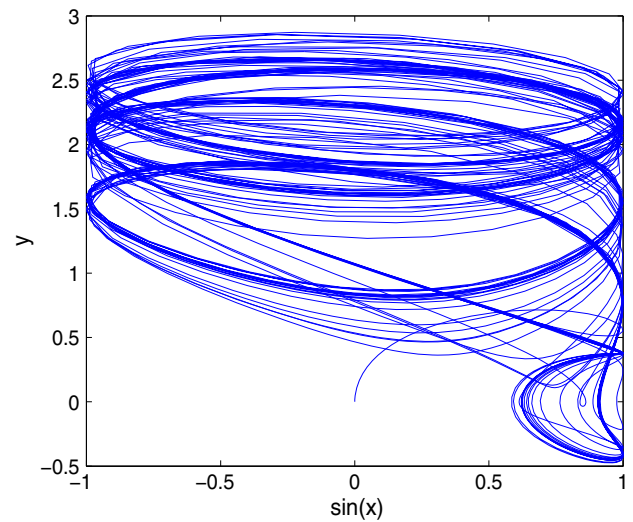


Fig. 2 Phase portrait of chaotic attractors of resistive-capacitive Josephson junction

as follows.

$$\begin{aligned} \dot{x} &= y \\ \dot{y} &= -\alpha y - \sin x + a + b \sin \omega t \end{aligned} \quad (3)$$

Figure 2 shows the chaotic attractor for resistive-capacitive shunted Josephson junction using the following parameter values: $\alpha = 0.5$, $a = 0.89$, $b = 0.4$ and $\omega = 0.25$.

3 Reduced order compound-synchronization scheme

In this section, compound synchronization scheme is designed for four chaotic systems based on the drive-response scheme. In this scheme, we shall consider three drive systems and one response systems.

The first drive system is given as

$$\dot{x} = f(x) \quad (4)$$

The second drive system is given as

$$\dot{y} = f(y) \quad (5)$$

The third drive system is given as

$$\dot{z} = f(z) \quad (6)$$

The response system is given as

$$\dot{w} = f(w) + u \quad (7)$$

where: $x = (x_1, x_2, \dots, x_m)^T$, $y = (y_1, y_2, \dots, y_n)^T$, $z = (z_1, z_2, \dots, z_p)^T$ and $w = (w_1, w_2, \dots, w_q)^T$ are the state

variables of systems (4)–(7) respectively; $f(x) \in \mathbb{R}^m$, $f(y) \in \mathbb{R}^n$, $f(z) \in \mathbb{R}^p$ and $f(w) \in \mathbb{R}^q$ are continuous functions of the systems; $u = (u_1, u_2, \dots, u_q)^T \in \mathbb{R}^q$ are controllers to be designed. We assume that $X = \text{diag}(x_1, x_2, \dots, x_m)$, $Y = \text{diag}(y_1, y_2, \dots, y_n)$, $Z = \text{diag}(z_1, z_2, \dots, z_p)$, and $W = \text{diag}(w_1, w_2, \dots, w_q)$ so we have the definition 1.

Definition 1 The drive systems (4)–(6) and the response systems (7) are said to achieve compound synchronization if there exists diagonal matrices $A \in \mathbb{R}^{m \times m}$, $B \in \mathbb{R}^{n \times n}$, $C \in \mathbb{R}^{p \times p}$, $D \in \mathbb{R}^{q \times q}$ and $D \neq 0$ where $m, n, p \geq q$ such that

$$\lim_{t \rightarrow \infty} \|e\| = \lim_{t \rightarrow \infty} \|DW - AX(BY + CZ)\| = 0 \quad (8)$$

where $\|\cdot\|$ represent the matrix norm, the constant matrices A, B, C and D are called scaling matrices and the drive system (4) is called the scaling drive system while the drive systems (5) and (6) are called the base drive systems.

Remark 1 m, n, p , and q are the orders of the drive systems and the response system.

Remark 2 If the scaling matrices $A \neq 0$, $B = 0$ or $C = 0$ then, the compound synchronization becomes a novel reduced order function projective combination synchronization where the scaling factor is a chaotic system which is different from the usual function projective synchronization scheme where the scaling matrix is usual a smooth function or a constant.

Remark 3 If the scaling matrices $A = B = C = 0$ then, the compound synchronization becomes chaos control problem (amplitude or oscillation death).

Remark 4 From definition 1 we can extend the number of drive chaotic systems to any number.

4 Generalized reduced-order compound synchronization of three third order and one second order chaotic Josephson junctions

4.1 Design of controllers via active backstepping technique

In this section, Josephson junctions in (9)–(11) are taken as the drive systems while the Josephson junction in (12) is taken as the response system in order to achieve generalized reduced order compound synchronization among the four chaotic Josephson junctions.

$$\begin{aligned} \dot{x}_1 &= x_2 \\ \dot{x}_2 &= \frac{1}{\beta_C} (i - g(x_2)x_2 - \sin x_1 - x_3) \\ \dot{x}_3 &= \frac{1}{\beta_L} (x_2 - x_3) \end{aligned} \quad (9)$$

$$\begin{aligned} \dot{y}_1 &= y_2 \\ \dot{y}_2 &= \frac{1}{\beta_C} (i - g(y_2)y_2 - \sin y_1 - y_3) \\ \dot{y}_3 &= \frac{1}{\beta_L} (y_2 - y_3) \end{aligned} \quad (10)$$

$$\begin{aligned} \dot{z}_1 &= z_2 \\ \dot{z}_2 &= \frac{1}{\beta_C} (i - g(z_2)z_2 - \sin z_1 - z_3) \\ \dot{z}_3 &= \frac{1}{\beta_L} (z_2 - z_3) \end{aligned} \quad (11)$$

$$\begin{aligned} \dot{w}_1 &= w_2 + u_1 \\ \dot{w}_2 &= -\alpha w_2 - \sin w_1 + a + b \sin \omega t + u_2 \end{aligned} \quad (12)$$

where u_1 and u_2 are the controllers to be designed. We define the error systems as follows

$$\begin{aligned} e_1 &= \delta_1 w_1 - \alpha_1 x_1 (\alpha_3 x_3 + \beta_1 y_1 + \beta_3 y_3 + \gamma_1 z_1 + \gamma_3 z_3) \\ e_2 &= \delta_2 w_2 - \alpha_2 x_2 (\beta_2 y_2 + \gamma_2 z_2) \end{aligned} \quad (13)$$

Differentiating (13) with respect to time yields the following error dynamics

$$\begin{aligned} \dot{e}_1 &= \delta_1 \dot{w}_1 - \alpha_1 \dot{x}_1 (\alpha_3 x_3 + \beta_1 y_1 + \beta_3 y_3 + \gamma_1 z_1 + \gamma_3 z_3) \\ &\quad - \alpha_1 x_1 (\alpha_3 \dot{x}_3 + \beta_1 \dot{y}_1 + \beta_3 \dot{y}_3 + \gamma_1 \dot{z}_1 + \gamma_3 \dot{z}_3) \\ \dot{e}_2 &= \delta_2 \dot{w}_2 - \alpha_2 \dot{x}_2 (\beta_2 y_2 + \gamma_2 z_2) - \alpha_2 x_2 (\beta_2 \dot{y}_2 + \gamma_2 \dot{z}_2) \end{aligned} \quad (14)$$

Substituting (9)–(12) into (14) yields

$$\begin{aligned} \dot{e}_1 &= \frac{\delta_1}{\delta_2} (e_2 + \alpha_2 x_2 (\beta_2 y_2 + \gamma_2 z_2)) \\ &\quad - \alpha_1 x_2 (\alpha_3 x_3 + \beta_1 y_1 + \beta_3 y_3 + \gamma_1 z_1 + \gamma_3 z_3) \\ &\quad - \alpha_1 x_1 \left(\frac{\alpha_3}{\beta_L} (x_2 - x_3) + \frac{\beta_3}{\beta_L} (y_2 - y_3) \right. \\ &\quad \left. + \frac{\gamma_3}{\beta_L} (z_2 - z_3) + \beta_1 y_2 + \gamma_1 z_2 \right) + \delta_1 u_1 \\ \dot{e}_2 &= -\alpha (e_2 + \alpha_2 x_2 (\beta_2 y_2 + \gamma_2 z_2)) \\ &\quad + \delta_2 (-\sin w_1 + a + b \sin \omega t) + \delta_2 u_2 \\ &\quad - \frac{\alpha_2}{\beta_C} (i - g(x_2)x_2 - \sin x_1 - x_3) (\beta_2 y_2 + \gamma_2 z_2) \\ &\quad - \alpha_2 x_2 \left(\frac{\beta_2}{\beta_C} (i - g(y_2)y_2 - \sin y_1 - y_3) \right. \\ &\quad \left. + \frac{\gamma_2}{\beta_C} (i - g(z_2)z_2 - \sin z_1 - z_3) \right) \end{aligned}$$

Consequently, the error dynamics can be written as

$$\begin{aligned} \dot{e}_1 &= \frac{\delta_1}{\delta_2} e_2 + A_1 + \delta_1 u_1 \\ \dot{e}_2 &= -\alpha e_2 + A_2 + \delta_2 u_2 \end{aligned} \quad (15)$$

where

$$\begin{aligned} A_1 &= \frac{\delta_1}{\delta_2} (\alpha_2 x_2 (\beta_2 y_2 + \gamma_2 z_2)) \\ &\quad - \alpha_1 x_2 (\alpha_3 x_3 + \beta_1 y_1 + \beta_3 y_3 + \gamma_1 z_1 + \gamma_3 z_3) \end{aligned}$$

$$\begin{aligned}
 & -\alpha_1 x_1 \left(\frac{\alpha_3}{\beta_L} (x_2 - x_3) + \frac{\beta_3}{\beta_L} (y_2 - y_3) \right. \\
 & \quad \left. + \frac{\gamma_3}{\beta_L} (z_2 - z_3) + \beta_1 y_2 + \gamma_1 z_2 \right) \\
 A_2 = & -\alpha_2 x_2 (\beta_2 y_2 + \gamma_2 z_2) + \delta_2 (-\sin w_1 + a + b \sin \omega t) \\
 & - \frac{\alpha_2}{\beta_C} (i - g(x_2)x_2 - \sin x_1 - x_3) (\beta_2 y_2 + \gamma_2 z_2) \\
 & - \alpha_2 x_2 \left(\frac{\beta_2}{\beta_C} (i - g(y_2)y_2 - \sin y_1 - y_3) \right. \\
 & \quad \left. + \frac{\gamma_2}{\beta_C} (i - g(z_2)z_2 - \sin z_1 - z_3) \right)
 \end{aligned}$$

then we have the following results

Theorem 1 *If the controllers are chosen as*

$$\begin{aligned}
 u_1 = & \frac{1}{\delta_1} \left(-\frac{\delta_1}{\delta_2} (\alpha_2 x_2 (\beta_2 y_2 + \gamma_2 z_2)) \right. \\
 & + \alpha_1 x_2 (\alpha_3 x_3 + \beta_1 y_1 + \beta_3 y_3 + \gamma_1 z_1 + \gamma_3 z_3) \\
 & + \alpha_1 x_1 \left(\frac{\alpha_3}{\beta_L} (x_2 - x_3) + \frac{\beta_3}{\beta_L} (y_2 - y_3) \right. \\
 & \quad \left. + \frac{\gamma_3}{\beta_L} (z_2 - z_3) + \beta_1 y_2 + \gamma_1 z_2 \right) - k q_1 \Big) \\
 u_2 = & \frac{1}{\delta_2} \left(\alpha_2 x_2 (\beta_2 y_2 + \gamma_2 z_2) - \delta_2 (-\sin w_1 + a + b \sin \omega t) \right. \\
 & - \frac{\delta_1}{\delta_2} + \frac{\alpha_2}{\beta_C} (i - g(x_2)x_2 - \sin x_1 - x_3) (\beta_2 y_2 + \gamma_2 z_2) \\
 & + (\alpha - k) q_2 + \alpha_2 x_2 \left(\frac{\beta_2}{\beta_C} (i - g(y_2)y_2 - \sin y_1 - y_3) \right. \\
 & \quad \left. + \frac{\gamma_2}{\beta_C} (i - g(z_2)z_2 - \sin z_1 - z_3) \right) \Big) \quad (16)
 \end{aligned}$$

where $q_1 = e_1$ and $q_2 = e_2$ then, the drive systems (9)–(11) will achieve generalized reduced order compound synchronization with the response systems (12).

Proof The objective of this paper is to find control functions via the active backstepping technique that would stabilize the error state dynamics (15) so that drive systems (9)–(11) and response system (12) achieve generalized reduced-order compound synchronization. The design procedures include the following steps.

Step 1 Let $q_1 = e_1$, its time derivative is

$$\dot{q}_1 = \dot{e}_1 = \frac{\delta_1}{\delta_2} e_2 + \delta_1 u_1 + A_1 \quad (17)$$

Where $e_2 = \alpha_1(q_1)$ can be regarded as virtual controller. In order to stabilize q_1 -subsystem, we choose a Lyapunov function $v_1 = \frac{1}{2} q_1^2$ and differentiating it with respect to time yields

$$\dot{v}_1 = q_1 \dot{q}_1 = q_1 \left(\frac{\delta_1}{\delta_2} \alpha_1(q_1) + A_1 + \delta_1 u_1 \right) \quad (18)$$

Suppose $\alpha_1(q_1) = 0$ and the control function u_1 is chosen as

$$u_1 = -\frac{1}{\delta_1} (A_1 + k q_1) \quad (19)$$

then $\dot{v}_1 = -k q_1^2 < 0$ where k is a positive constant which represents the feedback gain. Then, \dot{v}_1 is negative definite and the subsystem q_1 is asymptotically stable. Since, the virtual controller $\alpha_1(q_1)$ is estimative, the error between e_2 and $\alpha_1(q_1)$ is denoted by $q_2 = e_2 - \alpha_1(q_1)$ so, we have the (q_1, q_2) -subsystems

$$\begin{aligned}
 \dot{q}_1 &= \frac{\delta_1}{\delta_2} q_2 - k q_1 \\
 \dot{q}_2 &= -\alpha q_2 + \delta_2 u_2 + A_2
 \end{aligned} \quad (20)$$

Step 2 In order to stabilize subsystem (20) a Lyapunov function can be chosen as $v_2 = v_1 + \frac{1}{2} q_2^2$ and differentiating it with respect to time yields

$$\dot{v}_2 = -k q_1^2 + q_2 \left(\frac{\delta_1}{\delta_2} q_1 - \alpha q_2 + \delta_2 u_2 + A_2 \right) \quad (21)$$

If the control function u_2 is chosen as

$$u_2 = \frac{1}{\delta_2} \left(-A_2 - k q_2 + \alpha q_2 - \frac{\delta_1}{\delta_2} q_1 \right) \quad (22)$$

then $\dot{v}_2 = -k q_1^2 - k q_2^2 < 0$ where k is a positive constant which represents the feedback gain. Then, \dot{v}_2 is negative definite and the subsystem (q_1, q_2) in (20) is asymptotically stable. This implies that reduced order compound projective synchronization of the drive systems (9)–(11) and the response system (12) is achieved. Finally, the subsystem (20) becomes

$$\begin{aligned}
 \dot{q}_1 &= \frac{\delta_1}{\delta_2} q_2 - k q_1 \\
 \dot{q}_2 &= -\frac{\delta_1}{\delta_2} q_1 - k q_2
 \end{aligned} \quad (23)$$

so this complete the prove. \square

Remark 1 Different synchronization schemes can be obtained from this generalized control functions based on the choice of the scaling factors.

Remark 2 Several Corollaries can be obtained from Theorem 1 however, we shall limit ourselves to only few Corollaries needed in this paper. Note that the proofs of these Corollaries are similar to Theorem 1 so, they are omitted.

Let $\alpha_3 = \delta_1 = \delta_2 = \beta_1 = \beta_2 = \beta_3 = \gamma_1 = \gamma_2 = \gamma_3 = 1$ then, we have corollary 1.

Corollary 1 *If the controllers are chosen as*

$$\begin{aligned}
 u_1 = & \alpha_1 x_2 (x_3 + y_1 + y_3 + z_1 + z_3) - \alpha_2 x_2 (y_2 + z_2) - k q_1 \\
 & + \alpha_1 x_1 \left(\frac{1}{\beta_L} (x_2 - x_3) + \frac{1}{\beta_L} (y_2 - y_3) \right. \\
 & \quad \left. + \frac{1}{\beta_L} (z_2 - z_3) + y_2 + z_2 \right) \\
 u_2 = & \alpha_2 x_2 (y_2 + z_2) - (-\sin w_1 + a + b \sin \omega t) + (y_2 + z_2) \\
 & \times \frac{\alpha_2}{\beta_C} (i - g(x_2)x_2 - \sin x_1 - x_3)
 \end{aligned}$$

$$\begin{aligned}
& +\alpha_2 x_2 \left(\frac{1}{\beta_C} (i - g(y_2)y_2 - \sin y_1 - y_3) \right. \\
& \left. + \frac{1}{\beta_C} (i - g(z_2)z_2 - \sin z_1 - z_3) \right) \\
& + (\alpha - k)q_2 - q_1
\end{aligned} \quad (24)$$

where $q_1 = w_1 - \alpha_1 x_1(x_3 + y_1 + y_3 + z_1 + z_3)$, $q_2 = w_2 - \alpha_2 x_2(y_2 + z_2)$ then, the drive system (9)–(11) achieve reduced order modified projective compound synchronization with the response system (12).

Let $\alpha_3 = \delta_1 = \delta_2 = \beta_1 = \beta_2 = \beta_3 = \gamma_1 = \gamma_2 = \gamma_3 = 1$ then, we have corollary 2.

Corollary 2 If the controllers are chosen as

$$\begin{aligned}
u_1 &= \alpha_2 x_2(y_2 + z_2) - kq_1 \\
& - \alpha_1 x_2(\alpha_3 x_3 + \beta_1 y_1 + y_3 + z_1 + z_3) \\
& - \alpha_1 x_1 \left(\frac{1}{\beta_L}(x_2 - x_3) + \frac{1}{\beta_L}(y_2 - y_3) \right. \\
& \left. + \frac{1}{\beta_L}(z_2 - z_3) + y_2 + z_2 \right) \\
u_2 &= (\alpha - k)q_2 - q_1 - (\alpha \alpha_2 x_2(y_2 + z_2)) \\
& - (-\sin w_1 + a + b \sin \omega t) - (y_2 + z_2) \\
& \times \frac{\alpha_2}{\beta_C} (i - g(x_2)x_2 - \sin x_1 - x_3) \\
& - \alpha_2 x_2 \left(\frac{1}{\beta_C} (i - g(y_2)y_2 - \sin y_1 - y_3) \right. \\
& \left. + \frac{1}{\beta_C} (i - g(z_2)z_2 - \sin z_1 - z_3) \right)
\end{aligned} \quad (25)$$

where $q_1 = w_1 + \alpha_1 x_1(x_3 + y_1 + y_3 + z_1 + z_3)$, $q_2 = w_2 + \alpha_2 x_2(y_2 + z_2)$ then, the drive system (9)–(11) achieve reduced order modified projective compound anti-synchronization with the response system (12).

Let $\alpha_3 = \delta_1 = \delta_2 = \beta_1 = \beta_2 = \beta_3 = \gamma_1 = \gamma_2 = \gamma_3 = 1$ then, we have corollary 3.

Corollary 3 If the controllers are chosen as

$$\begin{aligned}
u_1 &= \alpha_2 x_2(y_2 + z_2) - kq_1 + \alpha_1 x_2(x_3 + y_1 + y_3 + z_1 + z_3) \\
& + \alpha_1 x_1 \left(\frac{1}{\beta_L}(x_2 - x_3) \right. \\
& \left. + \frac{1}{\beta_L}(y_2 - y_3) + \frac{1}{\beta_L}(z_2 - z_3) + y_2 + z_2 \right) \\
u_2 &= -\alpha \alpha_2 x_2(y_2 + z_2) \\
& - (-\sin w_1 + a + b \sin \omega t) - q_1 - (y_2 + z_2) \\
& \times \frac{\alpha_2}{\beta_C} (i - g(x_2)x_2 - \sin x_1 - x_3) \\
& - \alpha_2 x_2 \left(\frac{1}{\beta_C} (i - g(y_2)y_2 - \sin y_1 - y_3) \right. \\
& \left. + \frac{\gamma_2}{\beta_C} (i - g(z_2)z_2 - \sin z_1 - z_3) \right) + (\alpha - k)q_2
\end{aligned} \quad (26)$$

where $q_1 = w_1 - \alpha_1 x_1(x_3 + y_1 + y_3 + z_1 + z_3)$, $q_2 = w_2 + \alpha_2 x_2(y_2 + z_2)$ then, the drive system (9)–(11) achieve reduced

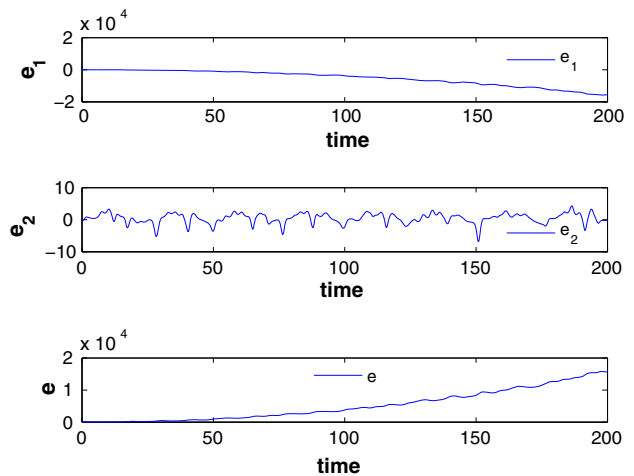


Fig. 3 Error dynamics of the drive and the response systems with controllers deactivated for $0 \leq t \leq 200$, where $e_1 = w_1 - 0.5x_1(y_1 + z_1)$, $e_2 = w_2 - 0.5x_2(y_2 + z_2)$ and $e = \sqrt{e_1^2 + e_2^2}$

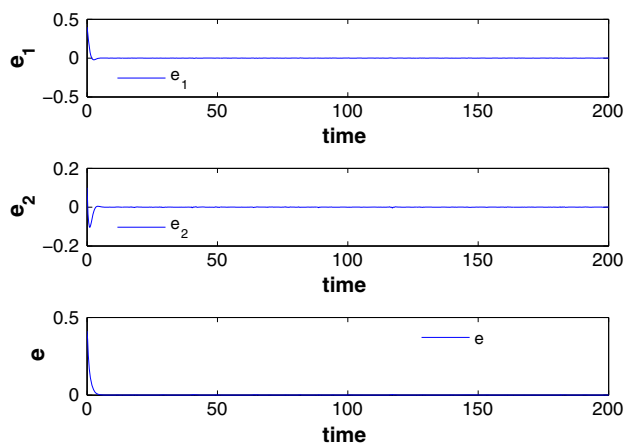


Fig. 4 Error dynamics of the drive and the response systems with controllers activated for $t \geq 0$, where $e_1 = w_1 - 0.5x_1(y_1 + z_1)$, $e_2 = w_2 - 0.5x_2(y_2 + z_2)$ and $e = \sqrt{e_1^2 + e_2^2}$

order modified projective compound hybrid synchronization with the response system (12).

4.2 Numerical simulation results

To validate the effectiveness of the designed controllers we used ode45 fourth order Runge–Kutta algorithm run on Matlab. In this numerical simulation procedure, the system parameter values are chosen to ensure chaotic dynamics of the state variables as shown in Figs. 1 and 2. The initial conditions of the drive systems and response system are chosen as $(x_1, x_2, x_3) = (0, 0, 0)$, $(y_1, y_2, y_3) = (1, 1, 1)$, $(z_1, z_2, z_3) = (0, 0, 0)$, $(w_1, w_2) = (1, 1)$. Now, the numerical simulation shall be considered under three cases.

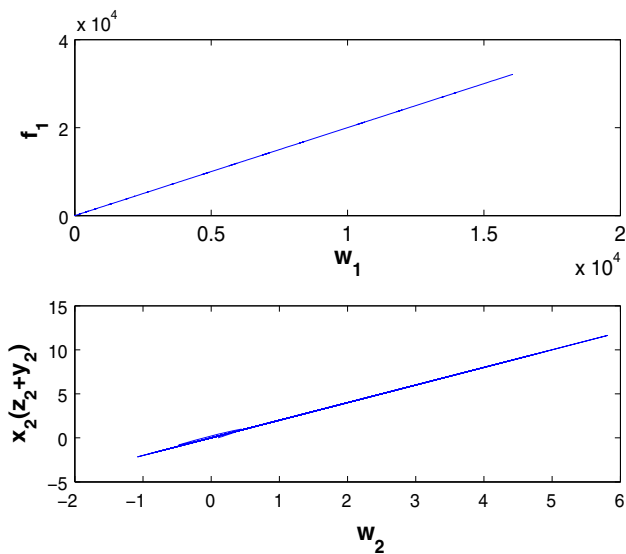


Fig. 5 Evidence of reduced order compound projective synchronization where $f_1 = x_1(x_3 + y_1 + y_3 + z_1 + z_3)$

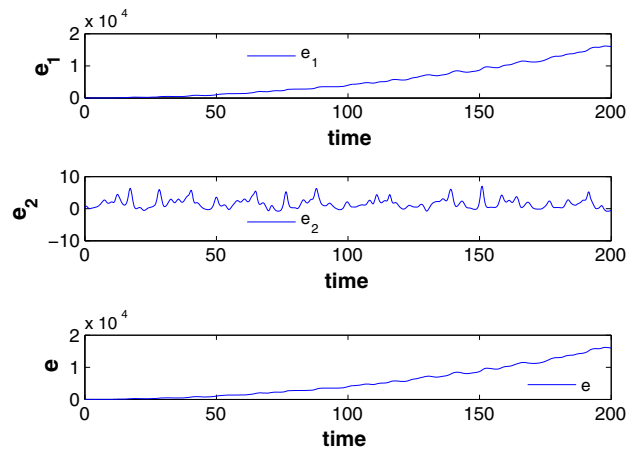


Fig. 6 Error dynamics of the drive and the response systems with controllers deactivated for $0 \leq t \leq 200$, where $e_1 = w_1 + 0.5x_1(y_1 + z_1)$, $e_2 = w_2 + 0.5x_2(y_2 + z_2)$ and $e = \sqrt{e_1^2 + e_2^2}$

Case 1 Let $\alpha_1 = \alpha_2 = 0.5$ in (24) then we have the following results: Fig. 3 shows the error dynamics of the state variables when the controllers are deactivated for $t \geq 0$; Fig. 4 shows that reduced order compound projective synchronization is achieved between the three drive JJs and the three response JJs as indicated by the convergence of the error dynamics of state variables to zero as soon as the controllers are switch on for $t \geq 0$. Figure 5 confirms the evidence of reduced order compound synchronization among the four chaotic Josephson junctions.

Case 2 Let $\alpha_1 = \alpha_2 = -0.5$ in (25) then we have the following results: Fig. 6 shows the error dynamics of the state variables when the controllers are deactivated for $t \geq 0$; Fig. 7 shows that reduced order compound projective

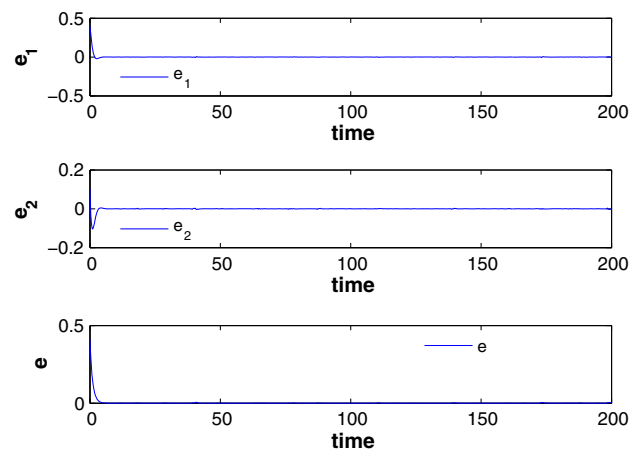


Fig. 7 Error dynamics of the drive and the response systems with controllers activated for $t \geq 0$, where $e_1 = w_1 + 0.5x_1(y_1 + z_1)$, $e_2 = w_2 + 0.5x_2(y_2 + z_2)$ and $e = \sqrt{e_1^2 + e_2^2}$

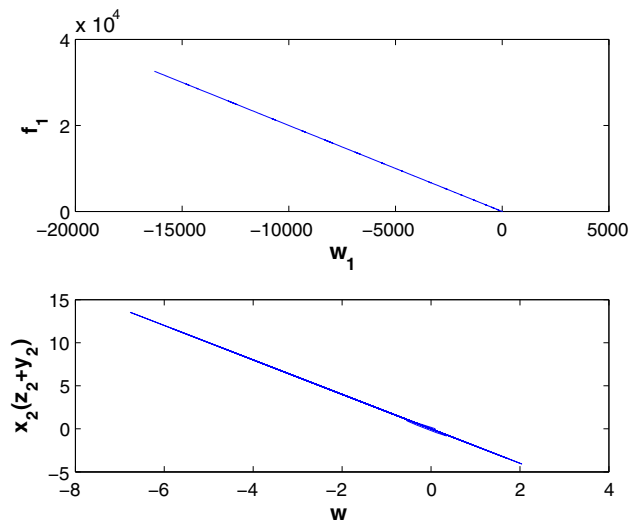


Fig. 8 Evidence of reduced order compound projective anti-synchronization where $f_1 = x_1(x_3 + y_1 + y_3 + z_1 + z_3)$

ive anti-synchronization is achieved between the three drive JJs and the three response JJs as indicated by the convergence of the error dynamics of state variables to zero as soon as the controllers are switch on for $t \geq 0$. Figure 8 confirms the evidence of reduced order compound projective anti-synchronization among the four chaotic Josephson junctions.

Case 3 Let $\alpha_1 = -0.5, \alpha_2 = 0.5$ in (26) then we have the following results: Fig. 9 shows the error dynamics of the state variables when the controllers are deactivated for $t \geq 0$; Fig. 10 shows that reduced order compound hybrid projective synchronization is achieved between the three drive JJs and the three response JJs as indicated by the convergence of the error dynamics of state variables to zero as soon as the controllers are switch on for $t \geq 0$. Figure 11 confirms

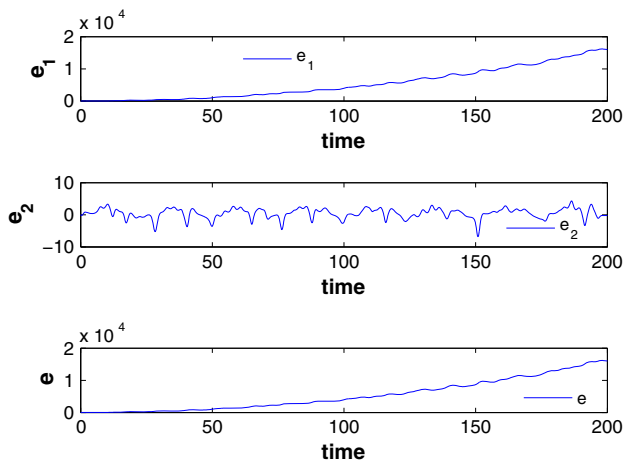


Fig. 9 Error dynamics of the drive and the response systems with controllers deactivated for $0 \leq t \leq 200$, where $e_1 = w_1 - 0.5x_1(y_1 + z_1)$, $e_2 = w_2 + 0.5x_2(y_2 + z_2)$ and $e = \sqrt{e_1^2 + e_2^2}$

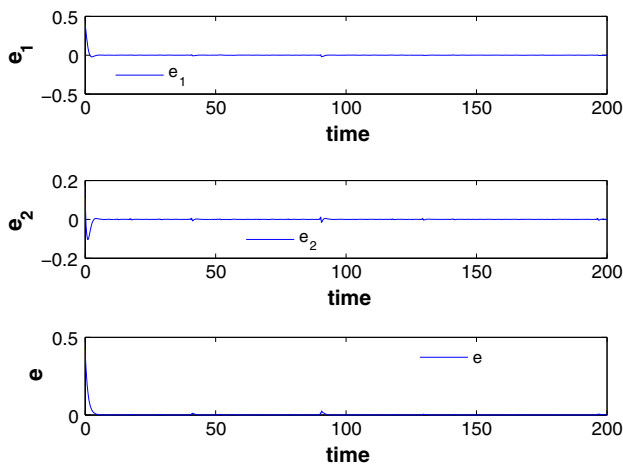


Fig. 10 Error dynamics of the drive and the response systems with controllers activated for $t \geq 0$, where $e_1 = w_1 - 0.5x_1(y_1 + z_1)$, $e_2 = w_2 + 0.5x_2(y_2 + z_2)$ and $e = \sqrt{e_1^2 + e_2^2}$

the evidence of reduced order compound hybrid projective synchronization among the four chaotic Josephson junctions.

5 Conclusion

Compound projective synchronization, compound projective anti-synchronization and compound projective hybrid synchronization of four chaotic Josephson junctions of different orders have been achieved using the active backstepping technique. The design procedure provides enough flexibility for one to choose any desired scaling factor which can be used to vary the output signal of the junctions to any desired level i.e to reduce or amplify the output signal. The scaling factors can also be varied to achieve any desired synchronization scheme

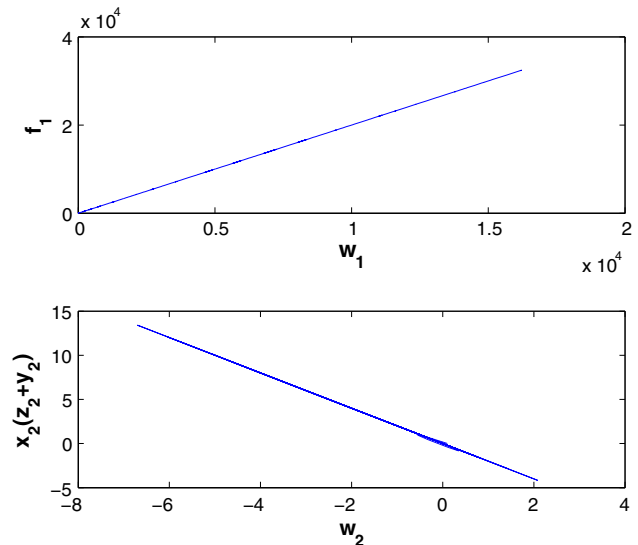


Fig. 11 Evidence of reduced order compound projective hybrid synchronization where $f_1 = x_1(x_3 + y_1 + y_3 + z_1 + z_3)$

(projective, anti-synchronization, generalized, hybrid, etc). Therefore, this new synchronization scheme could give better security to information transmission than other forms of synchronization due to its complexity in its formulation. It could also give a better insight into synchronization in biological systems since, synchronization in biological systems involves different organ of different dynamical structures and orders.

References

1. Zhou TG, Wang DC, Fang FL, Zhao XJ, Yan SL (2010) Simulation of chaos in different models of josephson junction. *J Syst Simul* 22:66–669
2. Gou R, Vincent UE, Idowu BA (2009) Synchronization of chaos in rcl-shunted josephson junction using a simple adaptive controller. *Phys Scr* 79:035801 (6pp)
3. Nayak CR, Kuriakose VC (2007) Dynamics of coupled josephson junctions under the influence of applied fields. *Phys Lett* 365:284–289
4. Kurt E, Canturk M (2009) Chaotic dynamics of resistively coupled dc-driven distinct josephson junctions and the effects of circuit parameters. *Phys D* 238(22):2229–2237
5. Yang XS, Li QD (2006) A computer-assisted proof of chaos in josephson junctions. *Chaos Solitons Fractals* 27(1):25–30
6. Kawaguchi T (2010) Directed transport and complex dynamics of vortices in a josephson junction network driven by modulated currents. *Phys C* 470(20):1133–1136
7. Idowu BA, Ucar A, Vincent UE (2009) Full and reduced-order synchronization of chaos in josephson junction. *AfrPhys Rev* 3:35–41
8. Njah AN, Ojo KS, Adebayo GA, Obawole AO (2010) Generalized control and synchronization of chaos in rcl-shunted josephson junction using backstepping design. *Phys C* 470:558–564
9. Hriscu AM, Nazarov YV (2013) Quantum synchronization of conjugated variables in a superconducting device leads to the fundamental resistance quantization. *Phys Rev Lett* 110:097002 (5pp)

10. Tian J, Qiu H, Wang G, Chen Y, Fu L-B (2013) Measure synchronization in a two species bosonic josephson junctions. *Phys Rev E* 88:032906–032908
11. Dana SK, Sengupta DC, Edoh KD (2001) Chaotic dynamics in josephson junction. *IEEE Trans Circuit Syst I Fundam Theory Appl* 48:990–996
12. Dana SK (2006) Spiking and bursting in josephson junction. *IEE Trans Circuits Syst II: Express Briefs* 53(10):1031–1034
13. Haken H (1994) Synergetics: from pattern formation to pattern analysis and pattern recognition. *Int J Bifurc Chaos Appl Sci Eng* 4:1069–1083
14. Yao C, Zhao Q, Yu J (2013) Complete synchronization induced by disorder in coupled chaotic lattice. *Phys Lett A* 377:370–377
15. Ojo KS, Njah AN, Adebayo GA (2011) Anti-synchronization of identical and non-identical ϕ^6 van der pol and ϕ^6 duffing oscillator with both parametric and external excitations via backstepping approach. *Int J Mod Phys B* 25(14):1957–1969
16. Sudheer KS, Sabir M (2009) Hybrid synchronization of hyperchaotic lu system. *Pramana* 73(4):781–786
17. Nian F, Wang X (2013) Projective synchronization of two different dimensional nonlinear systems. *Int J Mod Phys B* 27(21):1350113
18. Chen Y, Jia Z (2012) Hybrid projective dislocated synchronization of liu chaotic system based on parameters identification. *Mod Appl Sci* 6(2):16–21
19. Alsawalha MM, Noorani MSM (2012) Chaos reduced-order anti-synchronization of chaotic systems with fully unknown parameters. *Commun Nonlinear Sci Numer Simul* 17:1908–1920
20. Miao Q-Y, Fang J-A, Tang Y, Dong A-H (2009) Increase-order projective synchronization of chaotic systems with time delay. *Chin Phys Lett* 26(5):050501–(4pp)
21. Kareem SO, Ojo KS, Njah AN (2012) Function projective synchronization of identical and non-identical modified finance and shimizumorioka systems. *Pramana* 79(1):71–79
22. Runzi L, Yinglan W, Shucheng D (2011) Combination synchronization of three chaotic classic chaotic systems using active backstepping. *Chaos* 21:0431141–0431146
23. Wu Z, Fu X (2013) Combination synchronization of three different order nonlinear systems using active backstepping design. *Nonlinear Dyn* 73:1863–1872
24. Sun J, Shen Y, Zhang G, Xu C, Cui G (2013) Combination combination synchronization among four identical or different chaotic systems. *Nonlinear Dyn* 73:1211–1222
25. Lin H, Cai J, Wang J (2013) Finite-time combination-combination synchronization for hyperchaotic systems. *J Chaos* 2013:304643 (7pp)
26. Sun J, Shen Y, Yin Q, Xu C (2013) Compound synchronization of four memristor chaotic oscillator systems and secure communication. *Chaos* 23:013140
27. Ma M, Zhou J, Cai J (2012) Practical synchronization of nonautonomous systems with uncertain parameter mismatch via a single state feedback control. *Int J Mod Phys C* 23(11):12500731–1250073114
28. Yang CC (2011) Adaptive synchronization of lü hyperchaotic system with uncertain with parameters based on single-input controller. *Nonlinear Dyn* 63:447–454
29. Ojo KS, Njah AN, Ogunjo ST (2013) Comparison of backstepping and modified active control in projective synchronization of chaos in an extended bonhöffer- van der pol oscillator. *Pramana* 80(5):825–835
30. Njah AN, Ojo KS (2010) Backstepping control synchronization of parametrically and externally excited ϕ^6 oscillator with application to secure communication. *Int J Mod Phys B* 24(23):4581–4593
31. Yang CC (2012) Robust synchronization and anti-synchronization of identical ϕ^6 oscillators via adaptive sliding mode control. *J Sound Vib* 331:501–509
32. Padmanaban E, Banerjee R, Dana SK (2012) Targeting and control of synchronization in chaotic oscillators. *Int J Bifurc Chaos* 22(7):1250177 (12pp)
33. Wang J-W, Chen A-M (2010) A new scheme to projective synchronization of fractional-order chaotic systems. *Chin Phys Lett* 27(1):110501 (3pp)
34. Ricardo F, Gualberto SP (2002) Synchronization of chaotic systems with different order. *Phys Rev E* 65:036226
35. Stefanovska A, Haken H, McClintock PVE, Hozic M, Bajrovic CF, Ribaric S (2000) Reversible transitions between synchronization states of the cardiorespiratory system. *Phys Rev Lett* 85:4831–4834
36. Bowong S (2004) Stability analysis for the synchronization of chaotic system of different order: application to secure communications. *Phys Lett A* 326:102–113